Proc. Natl. Acad. Sci. USA
Vol. 86, pp. 5371–5375, July 1989
Biophysics

Mechanical properties of sensory hair bundles are reflected in their Brownian motion measured with a laser differential interferometer

(sacculus/fluctuation–dissipation theorem/viscous damping)

W. DENK*, W. W. WEBB*, AND A. J. HUDSPETH†

*School of Applied and Engineering Physics and Department of Physics, Cornell University, Ithaca, NY 14853; and †Department of Physiology, School of Medicine, University of California, San Francisco, CA 94143-0444

Communicated by E. E. Salpeter, April 3, 1989

ABSTRACT **By optically probing with a focused, low-power laser beam, we measured the spontaneous deflection fluctuations of the sensory hair bundles on frog saccular hair cells with a sensitivity of about 1 pm/$\sqrt{\text{Hz}}$. The preparation was illuminated by two orthogonally polarized laser beams separated by only about 0.2 μm at their foci in the structure under investigation. Slight movement of the object from one beam toward the other caused a change of the phase difference between the transmitted beams and an intensity modulation at the detector where the beams interfered. Maintenance of the health of the cells and function of the transduction mechanism were occasionally confirmed by measuring the intracellular resting potential and the sensitivity of transduction. The root-mean-square (rms) displacement of $\approx$3.5 nm at a hair bundle's tip suggests a stiffness of about 350 μN/m, in agreement with measurements made with a probe attached to a bundle's tip. The spectra resemble those of overdamped harmonic oscillators with roll-off frequencies between 200 and 800 Hz. Because the roll-off frequencies depended strongly on the viscosity of the bathing medium, we conclude that hair-bundle motion is mainly damped by the surrounding fluid.**

Central to the detection of acoustical and accelerational stimuli is the application of mechanical forces to the hair bundles of hair cells, the sensory receptors of the internal ear. When an appropriately oriented force is applied to the hair bundle, which consists of an elastically interconnected cluster of stereocilia protruding from a hair cell's apical surface, the bundle's resultant motion leads to the opening of mechanically sensitive transduction channels (for reviews see refs. 1 and 2). These channels are directly linked to elastic elements that are stretched by excitatory deflection of the hair bundle (3, 4).

Comprehension of the ear's operation mandates a thorough understanding of the hair bundle's mechanical properties for four reasons. (*i*) Because mechanoelectrical transduction by a hair cell commences with a mechanical input to the bundle, formulating a quantitative model of transduction requires that the bundle's mechanical impedance be known. (*ii*) Because the mechanical properties of hair bundles are the primary determinants of frequency selectivity in some hearing organs (5, 6), theories of tuning require detailed characterization of these properties (7). (*iii*) Because the mechanical properties of the bundle determine the extent of its Brownian (thermal) motion and because the noise source that limits the auditory system's performance is perhaps the transduction of Brownian motion (8), identification of the noise limits may depend upon measurements of the bundle's mechanical properties. (*iv*) Because mechanical feedback from hair cells may involve bundle motion (4, 9, 10), the bundle's ability to produce and transmit force is of interest.

The publication costs of this article were defrayed in part by page charge payment. This article must therefore be hereby marked "*advertisement*" in accordance with 18 U.S.C. §1734 solely to indicate this fact.

The mechanical properties of hair bundles have heretofore been studied quantitatively by displacing the bundles with elastic fibers of calibrated stiffness (9, 11, 12). Fibers have also been employed in the measurement of the bundles' Brownian motion and of changes in bundles' stiffness associated with transduction and adaptation (4, 10, 13, 14). The viscous drag on glass fibers impairs their responsiveness to rapid hair-bundle movements, however, and mechanical loading with a probe might affect active bundle motility as well. It would therefore be valuable to determine the mechanical properties of unperturbed hair bundles.

We describe here experiments in which, to avoid any interference stemming from probes, we measured the spontaneous motion of unencumbered hair bundles by optical differential interferometery (15). Such a measurement of the hair bundle's Brownian motion is well suited for investigation of the bundle's passive mechanical properties through their expression in spontaneous motion. It is also possible to search for active bundle movements at their lowest meaningful level, determined by the spectral density of thermal motion. Active processes are expected to manifest themselves as an excess of spontaneous motion, which, as in the case of spontaneous otoacoustic emissions (16), might be sharply tuned.

THEORY

The properties of the passive response of an object can be determined without actually stimulating the probed object by applying the equipartition and the fluctuation–dissipation theorems (17–19) to obtain unique relations between the variance and spectrum of equilibrium fluctuations of a quantity, such as velocity or electrical current, and the response of the same quantity to the corresponding external stimulus, such as force or voltage. The mechanical stiffness of a structure, such as the hair bundle, can be determined from the variance of its position fluctuations obtained as the integral over the power spectrum by the application of the equipartition theorem of statistical thermodynamics, which states that each degree of freedom contains $k_BT/2$ of energy. Here k_B is the Boltzmann constant and T is the absolute temperature. With x being the deflection from the average position, the mechanical stiffness (κ) is therefore

$$\kappa = k_BT/\langle x^2 \rangle.$$

Before we apply the fluctuation–dissipation theorem to the hair bundle we consider the diffusion of a free particle in a viscous fluid. The (one-sided) power spectral density (S_f^v) of the particle's velocity fluctuations is independent of the frequency (f) and is given by

$$S_f^v = 4k_BT/\gamma,$$

Abbreviation: DIC, differential-interference-contrast.

in which γ is the viscous drag. This relation is the mechanical analog of the thermal current noise S_f^I in a resistor R ($S_f^I = 4k_BT/R$). If we convert from velocities to deflections (x) and allow for a frequency-dependent compliance (c_f) defined as the response of the deflection (x_f) to a oscillating force (F_f) at the frequency f ($c_f = dx_f/dF_f$), we obtain

$$S_f^x = -\frac{2k_BT}{\pi f} Im(c_f),$$

in which $Im(c_f)$ denotes the imaginary part of the complex compliance.

If we assume linear behavior and that the restoring and damping forces affecting the hair bundle depend only on its instantaneous position and first time derivative, respectively, then the bundle can be mechanically modeled by a spring with stiffness κ in parallel with a dashpot (20) with damping strength γ. The compliance (c_f) then has a single pole and becomes

$$c_f = \frac{1}{\kappa(1 + i2\pi f\gamma/\kappa)}.$$

In this case, the mechanical state of the bundle is completely determined by a single parameter for each deflection direction and the power spectral density of the position fluctuations should have the form of a Lorentzian centered at zero frequency

$$\frac{d\langle x_f^2\rangle}{df} = \frac{4k_BT\gamma}{\kappa^2 + (2\pi f\gamma)^2}.$$

This function is flat for $2\pi f << \kappa/\gamma$ and declines as f^{-2} well above the roll-off frequency $f_k = \kappa/(2\pi\gamma)$. A change in the damping strength (γ) shifts the whole spectrum along a line with a slope of -1 in a double logarithmic plot. This scaling remains correct if the spectrum consists of a combination of Lorentzians for each of which the damping is changed by the same factor. Slope in this paper refers to the logarithmic slope; in plots of the logarithm of the power spectral density against the logarithm of the frequency, a function following a power law with exponent α appears as a straight line with slope α.

METHODS

All experiments were performed on hair cells of sacculi from American bullfrogs, *Rana catesbeiana*, with vent-to-snout lengths between 8 and 13 cm. The preparation of saccular macular epithelia was similar to that described elsewhere (21) but with the following variation: after the removal of the otoconia, additional digestion in a mixture of about 2 g of collagenase I per liter, 1 g of collagenase II per liter, and the usual 50 mg of subtilopeptidase per liter (Sigma) for 30–40 min allowed us to peel the sensory epithelium off its backing of nerves and connective tissue as well as to remove the otolithic membrane. The sheet of sensory cells was then clamped by a tungsten wire loop onto the coverslip forming the bottom of a small dish filled with saline solution (110 mM Na^+, 2 mM K^+, 4 mM Ca^{2+}, 118 mM Cl^-, 3 mM Hepes; pH 7.25). To observe the hair bundles by looking down upon their tips, we spread the cell sheet flat; to obtain a side view, we folded the sheet in such a way that the bundles of interest protruded horizontally.

The measurement of displacements was performed with what amounts to confocal differential-interference-contrast (DIC) microscopy by detecting the interference between two focused beams of laser light that traversed the sample along almost identical paths. Their diffraction-limited foci were each about 0.5 μm in diameter and their parallel axes were separated by $\approx$0.2 μm (Fig. 1). When an object that had a refractive index different from that of water moved between these foci, it increased its interaction with one beam while decreasing its interaction with the other beam. The relative phase of the two beams was consequently changed, causing an intensity change at the photodetector where the beams interfered (Fig. 2).

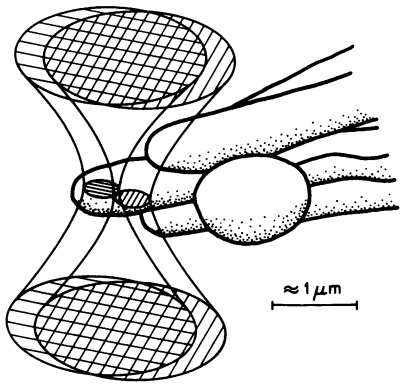

FIG. 1. Schematic drawing of the double focus of the two orthogonally polarized beams of the laser illumination when positioned to measure the displacement of the tallest stereocilium of a horizontally oriented hair bundle. The optical polarizations are indicated by the directions of shading.

Both beams were derived from a single He/Ne laser (4 mW at 633 nm) whose output was spatially filtered by transmitting it through an optical fiber to the microscope. The beam was split and recombined by modified Wollaston prisms (DIC sliders) provided by the microscope manufacturer (Zeiss) for its DIC system. Water-immersion microscope objectives (×40, numerical aperature = 0.75) were used to focus the beam pair onto the hair bundle, to collect the light, and to

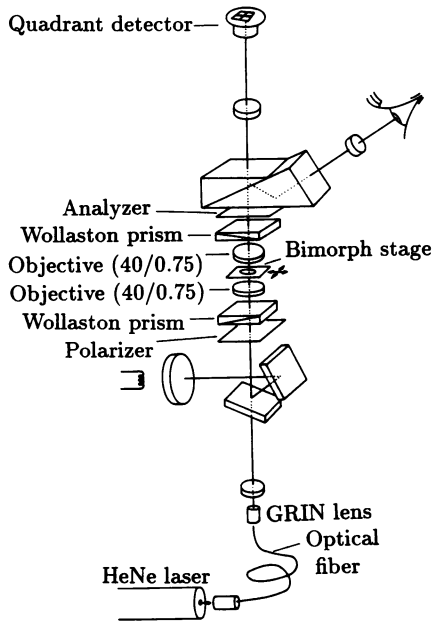

FIG. 2. Schematic diagram of the laser differential interferometer. An inverted microscope with regular DIC optics focuses the beam pair in the object, and an upright microscope, replacing the condenser, collects the light after it passes through the preparation, which is mounted in its dish on the piezoelectric-bimorph stage. To couple the laser light into and out of of the optical fiber, gradient index (GRIN) lenses are used in conjunction with micropositioners (Newport, Fountain Valley, CA). Simultaneous visual observation of the conventionally illuminated preparation and the attenuated laser beam allows us to assess very accurately the position of the focus within the structure of interest.

focus the recombined beams with total magnification of about ×1000 onto a quadrant photodetector (United Detector Technology, Hawthorne, CA). Even though in principle a single detector could be used, a quadrant detector allowed us to subtract and add the signals from opposing detector elements in order to make the experiment insensitive to intensity fluctuations of the illumination by dividing the difference by the sum. Low-noise amplification in the first stage combined with frequency compensation in a second stage (22) permitted us to work at the photon shot-noise limit for higher frequencies (>1 kHz). A modified apparatus has been devised, and is now used, that measures the ellipticity of the recombined light in a single spot limited by a pinhole.

A measurement of the total instrumentation noise spectrum is shown as the lowest trace in Fig. 3 on the same scale as typical data traces. The preprocessed signals were digitized by a dynamic signal analyzer (3562A; Hewlett–Packard) that also performed Fourier transforms, averaging, and power-spectrum calculations. Calibration of the electrical displacement signal was achieved by continuously moving the preparation with its dish in a circle 10 nm in diameter with a piezoelectric bimorph-driven stage (23). The imposed motion created a peak amplitude at its frequency (50 Hz) in each spectrum, which was subsequently used to normalize the trace. Through phase-sensitive detection of this signal component with a lock-in amplifier (124 A; Princeton Applied Research), we determined the exact direction of displacement sensitivity.

To change the viscosity of the extracellular fluid we dissolved large polysaccharide molecules (M_r = 500,000, Dextran T 500; Pharmacia) in the saline solution and measured the resulting viscosity with a capillary viscometer. Concentrations for changes in viscosities by factors of 3.2 and 10.1 were approximately 30 and 60 g/liter.

RESULTS

Hair-bundle motion was measured by positioning the double focus of the split laser beam somewhere in the topmost third of the bundle and then finely adjusting the position by a fraction of a micrometer to maximize the signal. Typical spectra are shown in Fig. 3. From the analysis of such spectra from 73 cells, we obtained a range of estimated rms values for the bundle displacement from 1 to 10 nm; the average value of 3.47 ± 1.5 nm (±SD) corresponds to a stiffness (κ) of 341 μN/m. Most roll-off frequencies lay between 200 and 800 Hz with a peak in the distribution at 450 Hz (Fig. 4).

Repeated measurement of the same bundle usually reproduced the rms displacement within ±1 nm and the roll-off frequency within ±100 Hz. The roll-off frequency and rms displacement were only slightly anticorrelated (correlation coefficient = −0.29). To obtain these values a simple Lorentzian was fitted by eye to the roll-off region of each spectrum (see Introduction). However, very few of the spectra showed a truly flat plateau below the roll-off frequency. Their slopes varied from −0.4 to −0.95 around a typical value of −0.7, and the slopes above the roll-off frequency were spread between −1.4 and −2.0. The values for rms deflection obtained by the fit of a Lorentzian are therefore smaller than what would have been obtained by simply integrating the spectrum, but the influence of background motion at very low and very high frequencies is avoided.

No significant difference could be found either between spectra taken in head-on and side-on positions or for motion along the excitatory direction of the bundle and perpendicular to it. Because of the spread in rms displacements and roll-off frequencies, however, an anisotropy factor of up to 1.3 could have gone undetected. It is possible that a bias was introduced due to the selection of larger bundles with high optical contrast.

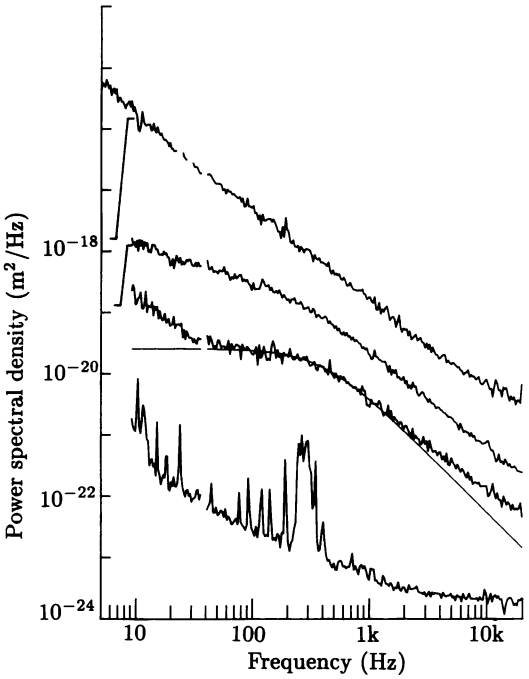

FIG. 3. Typical displacement power-spectral densities for (from the bottom to the top) the instrumental noise, a hair bundle with a nearly Lorentzian spectral shape (compare smooth Lorentzian trace), a hair bundle with the shape found most frequently, and a cell–cell boundary. All spectra were normalized by using the 50-Hz calibration peaks, which in this display are deleted for clarity. The topmost spectrum has been multiplied by a factor of 100 and the second from the top has been multiplied by a factor of 10 to avoid overlap. For each trace, Fourier transforms of 15–29 time series were averaged; the typical averaging time was <1 min. The raggedness of the traces is mainly due to the limited number of averages. The instrumental noise (lowest trace), measured by focusing on a latex bead embedded in agarose, is at the lowest frequencies probably due to building vibration that is not sufficiently attenuated by the vibration-isolation table. In the intermediate frequency range the influence of acoustical noise (mainly due to the cooling fan of the spectrum analyzer) becomes dominant, whereas at high frequencies only the photon shot noise, the fundamental limitation of any optical measurement, remains. The second trace from the bottom follows a Lorentzian spectral shape quite closely in the roll-off region with significant deviations above (even after removal of a constant background) and below the roll-off.

When in a few cases the position of the foci along the height of the stereocilia was varied, the amplitude, but not the shape, of the spectra changed. This result is consistent with bundle motion by pivoting of the stereocilia around their bases (9, 12).

Excess spontaneous motion, probably due to active processes, was observed in one cell (8). Because other accounts of such observations (9, 10, 13) indicate that this phenomenon is rare, spontaneous motion might not be typical of hair cell behavior.

To investigate the source of hair-bundle damping, we studied the influence of extracellular fluid viscosity. For three cells in three different preparations spectra were taken in standard saline, after the viscosity of the extracellular saline had been changed, and (for two of the three cells) again after the standard saline had been restored. The spectra changed mainly by shifting along the logarithmic frequency and amplitude axes toward lower frequencies and higher amplitudes in a way that left the rms amplitude unchanged. The shift factors along the frequency axis agreed, within the measurement errors, with the factors by which the viscosities had been changed (Table 1). After careful restoration of the original solution, the spectral shift was almost completely

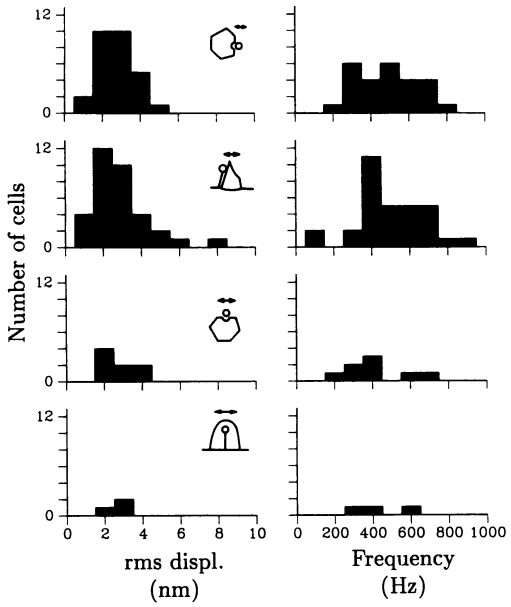

FIG. 4. Histograms of the distribution of roll-off frequencies and rms displacement amplitudes. The data obtained from 73 cells are sorted according to the bundle orientation relative to the illumination and direction of detected motion relative to the symmetry of the hair bundles (indicated by the sketches at the upper right corners of the individual histograms).

reversed. The single case for which the shift factor deviated significantly from the viscosity change factor may have been caused by incomplete fluid exchange.

To assess cellular health and functioning of the transduction mechanism we performed intracellular recordings on selected cells with high-resistance microelectrodes. Resting potentials ranged between −60 and −35 mV. For some cells transduction was measured as well by mechanically displacing the hair bundles or by correlating the bundle deflection fluctuations with the intracellular voltage fluctuations (8). We observed sensitivities between 3 kV/m and 400 kV/m, which is consistent with values published for such cells (21).

To compare the motion of other parts of the cell to that of the hair bundle we focused the measurement beams onto the boundary between a hair cell and an adjacent supporting cell. Although the resulting spectra showed rms amplitudes comparable to those of hair cells, they lacked the typical roll-off and instead followed a single-power law with fractional exponents around −1.5, in some cases over more than four decades of frequency. It is unlikely that this motion represents motion of the cell as a whole because the bounding membrane is likely to possess some freedom of motion on its own.

To test the measuring system, the Brownian motion of a flexible glass fiber immersed in distilled water was measured and found to be in excellent agreement with the predicted single-Lorentzian spectral shape.

Table 1. Changes in the values for spectral parameters as a result of a viscosity change

Cell no.	Relative viscosity (factor)	Frequency shift reduction (factor)*	Amplitude,* nm_{rms}
1	1	1.0 ± 0.2	4.0 ± 0.6
	3.5	3.5 ± 0.4	4.7 ± 0.5
	1	1.44 ± 0.1	5.4 ± 0.3
2	1	1.00 ± 0.07	2.5 ± 0.3
	3.18	3.2 ± 0.3	3.8 ± 0.3
	10.1	7.4 ± 0.7	3.3 ± 0.5
3	1	1.0	2.4
	10.1	9.9 ± 0.3	2.8 ± 1
	1	1.34 ± 0.19	1.9 ± 0.3

The first line for each cell gives the values before any viscosity change. Frequency-shift factors were measured relative to those first spectra and, as expected, agree roughly with the viscosity change factors, whereas the rms displacements do not vary systematically with viscosity. For cell nos. 1 and 3 reversibility data are given. Most values represent averages from the analysis of several spectra taken under identical conditions.
*Mean ± SD.

DISCUSSION

We have demonstrated that the Brownian motion of hair bundles and other cellular structures can be measured directly over a wide frequency range. As long as those structures can be observed with sufficient contrast in a DIC microscope, no extra particle or fiber needs to be attached. The passive mechanical properties of microscopic structures can thus be assessed without direct mechanical access by merely observing their motion as a result of thermal excitation.

For frog sacculi our results confirm measurements of hair-bundle stiffness using fine, elastic glass-fiber probes (10, 12). Furthermore, the shapes of the deflection–fluctuation spectra agree qualitatively with expectation from the simple model of an overdamped elastic structure. Instead of having the expected zero slope at low frequencies and the high frequency fall-off as f^{-2}, however, the typical hair-bundle spectrum shows a slope of −0.7 below and −1.7 above the roll-off frequency. This suggests a whole distribution of relaxation times, peaked around the inverse of the roll-off frequency, due to a collection of modes of internal motion. To test this hypothesis simultaneous measurements at different locations of the bundle are necessary. Because the transduction process is thought to involve the opening and closing of mechanically gated channels, one expects the existence of internal degrees of freedom that affect the deflection. Such channels would change their dimensions while switching between open and closed states (4). Since it is likely that these channels are located at or near the tips of the stereocilia (24), the length of connections between stereocilia could be affected so that displacement of the whole bundle would ensue. It is tempting to attribute the upturn seen at low frequencies for some cells (Fig. 3) to the mechanical adaptation mechanism (10), but low-frequency background noise and possible cell body motion make this conclusion uncertain.

The origin of hair-bundle damping has been identified. Its dependence on the viscosity of the bathing fluid proves that it is almost entirely due to shear flow in the extracellular medium and not to viscoelastic cellular structures. It must be borne in mind in this case that the hair bundles in the frog sacculus are not naturally freestanding but are normally connected to the otolithic membrane. As the same viscosity dependence is very likely to apply to the case of naturally freestanding hair bundles such as those in the inner hair cells of the mammalian cochlea and in the lizard basilar papilla (5–7), this property maximizes the mechanical signal-to-noise ratio because in those hair cells the stimulus is viscously coupled to the bundle. It is also interesting to compare the damping of the hair bundle with the Stokes drag of a solid sphere of similar dimensions whose drag coefficient (γ_s) is given by $\gamma_s = 6\pi\eta a$, in which η is the viscosity and a is the radius of the sphere. For a sphere 5 μm in diameter we obtain in water γ_s = 47 nNs/m. The damping for the hair bundles [$\gamma_{hb} = \kappa/(2\pi f_k)$], calculated using the average values for stiffness and roll-off frequency, is γ_{hb} = 127 nNs/m, which is significantly larger than the theoretical value for a sphere of similar dimensions. This was expected because of the relative shear motion that occurs between stereocilia as a

result of bundle deflection. A similar value was also obtained by measurements of a bundle's Brownian motion when attached to a glass-fiber probe (14).

This research was supported by grants from the National Institutes of Health (GM33028 and NS20429) and from the National Science Foundation (DMB8609084), by an equipment grant from AT&T, and by an IBM graduate fellowship to W.D.

1. Howard, J., Roberts, W. M. & Hudspeth, A. J. (1988) *Annu. Rev. Biophys. Biophys. Chem.* **17**, 99–124.
2. Roberts, W. M., Howard, J. & Hudspeth, A. J. (1988) *Annu. Rev. Cell Biol.* **4**, 63–92.
3. Corey, D. P. & Hudspeth, A. J. (1983) *J. Neurosci.* **3**, 962–976.
4. Howard, J. & Hudspeth, A. J. (1988) *Neuron* **1**, 189–199.
5. Frishkopf, L. S. & DeRosier, D. J. (1983) *Hearing Res.* **12**, 393–404.
6. Holton, T. & Hudspeth, A. J. (1983) *Science* **222**, 508–510.
7. Weiss, T. F. & Leong, R. (1985) *Hearing Res.* **20**, 157–174.
8. Denk, W. & Webb, W. W. (1989) in *Cochlear Mechanics, Structure, Function and Models*, eds. Wilson, J. P. & Kemp, D. T. (Plenum, New York), pp. 125–134.
9. Crawford, A. C. & Fettiplace, R. (1985) *J. Physiol. (London)* **364**, 359–379.
10. Howard, J. & Hudspeth, A. J. (1987) *Proc. Natl. Acad. Sci. USA* **84**, 3064–3068.
11. Flock, Å. & Strelioff, D. (1984) *Nature (London)* **310**, 597–599.
12. Howard, J. & Ashmore, J. F. (1986) *Hearing Res.* **23**, 93–104.
13. Howard, J. & Hudspeth, A. J. (1987) in *Sensory Transduction*, Report of the 1987 FESN Study Group: Discussions in Neurosciences, eds. Hudspeth, A. J., MacLeish, P. R., Margolis, F. L. & Wiesel, T. N. (Fondation pour l'Etude du Système Nerveux Central et Pèriphérique, Geneva), Vol. 4, pp. 138–145.
14. Howard, J. & Hudspeth, A. J. (1987) *Biophys. J.* **51**, 203a (abstr.).
15. Denk, W., Hudspeth, A. J. & Webb, W. W. (1986) *Biophys. J.* **49**, 21a (abstr.).
16. Zurek, P. M. (1981) *J. Acoust. Soc. Am.* **69**, 514–523.
17. Callen, H. B. & Welton, T. A. (1951) *Phys. Rev.* **83**, 34–40.
18. Landau, L. D. & Lifshitz, E. M. (1980) *Course of Theoretical Physics* (Pergamon, New York), Vol. 6.
19. Reichl, L. E. (1980) *A Modern Course in Statistical Physics* (Univ. of Texas, Austin).
20. Hudspeth, A. J. (1985) in *Contemporary Sensory Neurobiology*, eds. Correia, M. J. & Perachio, A. A. (Liss, New York), pp. 193–205.
21. Hudspeth, A. J. & Corey, D. P. (1977) *Proc. Natl. Acad. Sci. USA* **74**, 2407–2411.
22. Sigworth, F. (1983) in *Single-Channel Recording*, eds. Sackmann, B. & Neher, E. (Plenum, New York), pp. 3–35.
23. Muralt, P., Pohl, D. W. & Denk, W. (1986) *IBM J. Res. Dev.* **30**, 443–450.
24. Hudspeth, A. J. (1982) *J. Neurosci.* **2**, 1–10.